Requirement for TRanslocon-Associated Protein (TRAP) α in insulin biogenesis

Xin Li[*1], Omar A. Itani[*2,3], Leena Haataja[2,4], Kathleen J. Dumas[2,3], Jing Yang[1], Jeeyeon Cha[5,8], Stephane Flibotte[9], Hung-Jen Shih[3], Jialu Xu[1], Ling Qi[2,4], Peter Arvan[2,4], Ming Liu[#1,2,4], and Patrick J. Hu[#2,3,5,6,7]

[1]Department of Endocrinology and Metabolism, Tianjin Medical University General Hospital, Tianjin, China

[2]Departments of Internal Medicine and [3]Cell and Developmental Biology, and [4]Division of Metabolism, Endocrinology & Diabetes, University of Michigan Medical School, Ann Arbor, MI

[5]Departments of Medicine and [6]Cell and Developmental Biology, [7]Division of Hematology and Oncology, and [8]Division of Diabetes, Endocrinology & Metabolism, Vanderbilt University Medical Center, Nashville, TN

[9]Department of Zoology and Michael Smith Laboratories, University of British Columbia, Vancouver, British Columbia

[*]These authors contributed equally to this work

[#]Co-corresponding authors

The mechanistic basis for the biogenesis of peptide hormones and growth factors is poorly understood. Here we show that the conserved endoplasmic reticulum (ER) membrane translocon-associated protein (TRAP) α, also known as signal sequence receptor 1 (SSR1)[1], plays a critical role in the biosynthesis of insulin. A genetic screen in the nematode *Caenorhabditis elegans* revealed *trap-1*, which encodes the *C. elegans* TRAPα ortholog, as a modifier of DAF-2 insulin receptor (InsR) signaling. Genetic analysis indicates that TRAP-1 acts upstream of DAF-2/InsR to control *C. elegans* development. Endogenous *C. elegans* TRAP-1 and mammalian TRAPα both localized to the ER. In pancreatic beta cells, TRAPα deletion impaired preproinsulin translocation but did not affect the synthesis of α_1-antitrypsin, indicating that TRAPα selectively influences the translocation of a subset of secreted proteins. Surprisingly, loss of TRAPα function also resulted in disruption of distal steps in insulin biogenesis including proinsulin processing and secretion. These results show that TRAPα assists in the ER translocation of preproinsulin and unveil unanticipated additional consequences of TRAPα loss-of-function on the intracellular trafficking and maturation of proinsulin. The association of common intronic single nucleotide variants in the human TRAPα gene with susceptibility to Type 2 diabetes and pancreatic beta cell dysfunction[2] suggests that impairment of preproinsulin translocation and proinsulin trafficking may contribute to the pathogenesis of Type 2 diabetes.

The *C. elegans* DAF-2/InsR pathway prevents dauer diapause through a conserved phosphoinositide 3-kinase (PI3K)/Akt pathway that inhibits the FoxO transcription factor DAF-16. In the context of reduced DAF-2/InsR signaling, cytoplasmic DAF-16/FoxO

translocates to the nucleus and promotes dauer arrest through transcriptional regulation[3,4]. In a genetic screen for suppressors of the dauer-constitutive phenotype of an *eak-7;akt-1* double mutant strain that exhibits reduced DAF-2/InsR signaling and increased DAF-16/FoxO activity[5-8], we isolated a strain containing a ~3.5 kb deletion, *dpDf665,* that spanned the *trap-1* gene as well as three exons of the upstream gene Y71F9AL.1 (Figure 1A). Three independent *trap-1* null mutations (Figure S1) phenocopied the *dpDf665* deletion (Figure 1B), whereas a null mutation in Y71F9AL.1 did not (Figure S2), indicating that the mutant phenotype is a consequence of *trap-1* deletion. *trap-1* mutation suppressed the dauer-constitutive phenotype of mutants with reduced DAF-2/InsR signaling (Figure 1C) but not the phenotype of mutants with reduced signaling in other pathways that inhibit dauer diapause[3,9] (Figure S3). Furthermore, *trap-1* mutation impaired the induction of DAF-16/FoxO target genes caused by DAF-2/InsR mutation[10] (Figures 1D-F). Thus, TRAP-1 promotes dauer arrest by specifically antagonizing the DAF-2/InsR pathway.

TRAP-1 is orthologous to mammalian TRAPα/SSR1 (henceforth referred to as "TRAPα"), a transmembrane ER protein identified based on its interaction with the preprolactin signal peptide during *in vitro* protein translocation[1,11] (Figure S4). TRAPα physically associates with three other conserved ER transmembrane proteins (TRAPβ, γ, and δ) to form the TRAP complex[12]. A functional single-copy TRAP-1::mCherry fusion protein generated by CRISPR/Cas9-mediated knock-in (Figure 1C) is expressed in several tissues in *C. elegans* embryos, larvae, and adult animals (Figures 2A-C). Coexpression of

63 TRAP-1::mCherry with the ER protein signal peptidase fused to GFP[13] revealed that
64 endogenous TRAP-1 localizes to the ER (Figure 2D).

65 Although the biological function of mammalian TRAPα has not been established, it is
66 thought to play a role in cotranslational ER translocation based on its interaction with the
67 preprolactin signal peptide *in vitro*[11], its necessity for the *in vitro* translocation of prion
68 protein[14], and its physical proximity to the Sec61 protein translocation channel[15-19]. As the
69 expanded *C. elegans* insulin-like gene family encodes 40 peptides, some of which enhance
70 dauer arrest by antagonizing DAF-2/InsR signaling[20,21], we hypothesized that TRAP-1
71 influences DAF-2/InsR signaling by promoting the ER-based biosynthesis of one or more of
72 these insulin-like negative regulators of DAF-2/InsR[20]. If this model is correct, then DAF-
73 2/InsR mutations that impair receptor function downstream of ligand binding should be
74 resistant to suppression by *trap-1* mutation, as these mutant DAF-2/InsR receptors would be
75 refractory to changes in ligand-mediated activity caused by *trap-1* mutation. We therefore
76 tested the effect of *trap-1* mutation on the dauer-constitutive phenotype of eight distinct *daf-*
77 *2/InsR* loss-of-function alleles, seven of which affect amino acid residues that are conserved
78 in the human InsR[22] (Table S1).

79 Whereas *trap-1* mutation suppressed the dauer-constitutive phenotype of the *daf-2*
80 alleles *e1368* and *m212* (Figure S5A and Table S1), both of which encode receptors with
81 missense mutations in the extracellular ligand-binding domain[22,23], the dauer-constitutive
82 phenotypes of the other six *daf-2* alleles were not affected by *trap-1* mutation. The functional
83 consequences of four of these six DAF-2/InsR mutations can be inferred from data on human

84 InsRs with point mutations affecting the corresponding conserved residues (Table S1). A
85 heterozygous mutation in the human InsR kinase domain corresponding to *daf-2(e1391)*[23]
86 was found in a patient with autosomal dominant Type A insulin-resistant diabetes mellitus
87 with acanthosis nigricans (IRAN)[24] and results in a severe reduction in InsR *in vitro* kinase
88 activity and autophosphorylation[25]. Another Type A IRAN patient was found to be
89 homozygous for a missense mutation in the InsR extracellular domain corresponding to *daf-*
90 *2(m579)*[26] that reduces the affinity of InsR for insulin by three-to-five fold[27]. A missense
91 mutation affecting the conserved residue in the human InsR corresponding to the glycine
92 mutated in *daf-2(m596)* was identified in a patient with insulin resistance and
93 leprechaunism[28] and reduces the amount of InsR present at the plasma membrane by more
94 than 90%[29]. Finally, human InsR harboring a missense mutation affecting the conserved
95 cysteine mutated in *daf-2(m577)*[22] exhibits a 100-fold reduction in levels of mature
96 tetrameric receptor present at the cell surface compared to wild-type human InsR[30]. The
97 failure of *trap-1* mutation to suppress the dauer-constitutive phenotypes of these *daf-2/InsR*
98 alleles (Figure S5A and Table S1) indicates that TRAP-1 acts upstream of DAF-2/InsR and is
99 consistent with a role for TRAP-1 in the biogenesis of insulin-like peptide ligands that
100 antagonize DAF-2/InsR.

101 To further test the hypothesis that TRAP-1 promotes the biogenesis of antagonistic
102 DAF-2/InsR ligands, we determined the effect of *trap-1* mutation on the dauer-constitutive
103 phenotype of animals with mutations in three genes encoding DAF-2/InsR agonist peptides[21].
104 *trap-1* mutation partially suppressed the dauer-constitutive phenotype of *ins-4 ins-6;daf-28*

105 triple mutants (Figure S5B), consistent with a model whereby TRAP-1 promotes antagonist
106 insulin-like peptide ligand action.

107 As human insulin antagonizes DAF-2/InsR signaling when it is expressed in *C.*
108 *elegans*[20], we explored the possibility that mammalian TRAPα promotes insulin biogenesis.
109 Endogenous TRAPα colocalized with KDEL ER resident proteins but not with the Golgi
110 marker GM130[31] in rat INS 832/13 pancreatic beta cells (Figure 3A). To assess the role of
111 TRAPα in preproinsulin translocation, we generated INS 832/13 cells lacking TRAPα using
112 CRISPR/Cas9-based genome editing. Normally, preproinsulin is nearly undetectable by
113 immunoblotting with anti-proinsulin antibodies (Figure 3B, first two lanes), but TRAPα
114 knockout (KO) resulted in detectable amounts of preproinsulin (Figure 3B, third lane) that
115 increased further upon pretreatment of cells with the proteasome inhibitor MG132 (Figure
116 3B, last lane).

117 These data could be consistent with a requirement for TRAPα in the translocation of
118 preproinsulin such that in the absence of TRAPα, untranslocated preproinsulin is degraded
119 by the proteasome. Alternatively, the data in Figure 3B could be consistent with impaired
120 preproinsulin processing by signal peptidase in the ER. To distinguish between a
121 translocation defect and a signal peptidase processing defect in TRAPα KO cells, we
122 determined the protease sensitivity of preproinsulin in TRAPα KO cells after selective
123 permeabilization of the plasma membrane (Figure 3C). In wild-type cells, preproinsulin was
124 fully translocated into the ER and processed to proinsulin that was protease-resistant after
125 plasma membrane permeabilization with digitonin but degraded after full solubilization of

internal membranes with Triton X-100 (Figure 3C, third and fourth lanes). In TRAPα KO cells, accumulated preproinsulin was protease-sensitive both after partial as well as complete membrane permeabilization (Figure 3C, seventh and eighth lanes). These data indicate that in TRAPα KO cells, preproinsulin remains untranslocated in the cytosol.

While the steady-state level of proinsulin was not affected by TRAPα KO (Figures 3B and 3C), anti-insulin immunoblotting revealed a surprisingly dramatic reduction in total insulin content in TRAPα KO cells compared to control cells (Figure 3D). TRAPα knockdown by RNAi recapitulated this decrease in steady-state insulin levels (Figure 3E), indicating that this phenotype does not represent an off-target effect of genome editing.

To gain further insight into the role of TRAPα in early events governing insulin biogenesis, we pulse-labeled cells with ^{35}S-labeled methionine and cysteine (^{35}S-Met/Cys) and analyzed insulin biosynthetic intermediates by immunoprecipitation immediately after labeling or after a chase of 60 or 120 minutes (Figures 3F-H). In wild-type cells, proinsulin (PI) was efficiently labeled with ^{35}S-Met/Cys (Figure 3F, lane 1) and processed into mature insulin (Ins-B; lanes 2 and 4). Additionally, both proinsulin and insulin were secreted into the media (M; lanes 3 and 5). Notably, in wild-type cells, preproinsulin (pPI) was not detected, consistent with its rapid translocation and conversion to proinsulin in the ER. In contrast, in TRAPα KO cells, newly synthesized preproinsulin was detectable immediately after labeling (lane 6) but was lost thereafter. While proinsulin was still synthesized (lane 6), its recovery at 60 and 120 minutes after labeling was diminished (compare lanes 7 and 9 to lane 6), and proinsulin was neither secreted intact nor processed to mature insulin

147 intracellularly (lanes 7-10). Therefore, in addition to impairing preproinsulin ER
148 translocation, TRAPα KO also results in reduced proinsulin stability, with dramatically
149 decreased insulin biogenesis and secretion.

150 To elucidate the contribution of the proteasome to increased proinsulin turnover in
151 TRAPα KO cells, we treated ^{35}S-Met/Cys-labeled cells with the proteasome inhibitor MG132.
152 MG132 treatment increased intracellular proinsulin levels (Figure S6, compare lane 13 to
153 lane 11 and lane 17 to lane 15). However, this increase did not rescue defects in proinsulin
154 secretion and processing to mature insulin. Therefore, TRAPα KO impairs the intracellular
155 trafficking of proinsulin and the biogenesis of insulin independent of its effect on proinsulin
156 turnover.

157 To determine whether the proinsulin trafficking defect observed in TRAPα KO cells
158 was due to a general defect in the secretory pathway, we analyzed the biogenesis and
159 secretion of α1-antitrypsin (AAT) in wild-type and TRAPα KO cells. TRAPα KO affected
160 neither the biogenesis nor the secretion of AAT (Figures 3I-J). These findings indicate that
161 the secretory pathway is functionally intact in TRAPα KO cells and also demonstrate that
162 TRAPα promotes the ER translocation and subsequent trafficking of only a subset of secreted
163 proteins.

164 We also used immunofluorescence to independently examine the consequences of
165 TRAPα KO on insulin biogenesis. In wild-type cells, insulin (Figure 4A) and proinsulin
166 (Figure 4B) were readily detectable. However, TRAPα KO resulted in a dramatic decrease in
167 insulin content (Figure 4A), although proinsulin was still detectable (Figure 4B).

Reintroducing epitope-tagged TRAPα into TRAPα KO cells rescued insulin production in transfected cells (Figures 4C-D), and infection of TRAPα KO cells with adenovirus encoding TRAPα at increasing multiplicities of infection revealed that this rescue was dose-dependent (Figure S7).

Our finding that TRAPα activity is required for efficient insulin biogenesis and secretion was unexpected. Defects in proinsulin processing and secretion could be an indirect consequence of TRAPα dysfunction in the ER. In mouse fibroblasts, TRAPα physically associates with misfolded ER-associated degradation (ERAD) substrates[32], suggesting that TRAPα may play a role in reducing ER stress. Thus, in pancreatic beta cells, loss of TRAPα may cause abnormalities in proinsulin processing and secretion (Figures 3F-H) due to a general increase in ER stress.

To determine whether *C. elegans* TRAP-1 and mammalian TRAPα play roles in mitigating ER stress, we assayed for constitutive activation of the unfolded protein response in animals and beta cells lacking TRAP-1 or TRAPα, respectively. In *C. elegans,* transcription of *hsp-4,* which encodes a homolog of the human ER chaperone BiP, is induced by ER stress[33]. Indeed, while green fluorescence was not detectable in wild-type *hsp-4*::GFP reporter animals grown under normal culture conditions, it was readily visualized in *trap-1* mutant animals harboring the same transgene (Figure 4E). Similarly, increased phosphorylation of eIF2α at serine 51, which is phosphorylated by PERK in response to ER stress[34], was detected in INS 832/13 cells with reduced TRAPα expression but not in wild-type INS 832/13 cells (Figure 4F). Thus, we cannot exclude the possibility that TRAPα may

189 indirectly influence distal events in insulin biogenesis through effects on ER stress that are
190 not similarly consequential for α1-antitrypsin (Figures 3I-J).

191 Although the role of ER translocation in governing insulin biogenesis has been
192 underappreciated, hints of its importance have emerged from studies on rare missense
193 mutations in the signal peptide of human preproinsulin that are associated with congenital
194 diabetes[35]. The current work provides insight into the importance of the ER translocation
195 machinery in insulin biogenesis by establishing preproinsulin as the first bonafide client
196 protein for TRAPα. Our data are consistent with a model whereby TRAPα directly promotes
197 preproinsulin translocation and indirectly influences proinsulin maturation and insulin
198 secretion, possibly through its effects on ER stress. Variation in TRAPα expression and/or
199 activity may be generally relevant to the pathogenesis of Type 2 diabetes, as several common
200 intronic single nucleotide variants in the human *Ssr1* gene (encoding TRAPα) are associated
201 with Type 2 diabetes risk and pancreatic beta cell dysfunction[2]. Intriguingly, genes encoding
202 TRAP subunits are among the most highly upregulated genes in pancreatic beta cells exposed
203 to high glucose concentrations[36], and the transcriptional induction of TRAPα, β, and γ in
204 pancreatic beta cells requires the unfolded protein response transducer IRE1α[37]. Thus,
205 upregulation of TRAPα in pancreatic beta cells in the context of hyperglycemia may
206 promote metabolic stability by both enhancing insulin biogenesis and attenuating ER stress.
207 Understanding the mechanistic basis for TRAPα action in insulin biogenesis may lead to new
208 approaches to prevent and treat Type 2 diabetes.

As mammalian TRAPα is expressed widely[38], it surely must have biological functions that are distinct from its role in insulin biogenesis. These may include promoting the translocation of other proteins that enter the secretory pathway (such as PrP[14]) and/or participating in ERAD[32]. Mice homozygous for a C-terminal TRAPα-*ShBle-LacZ* fusion allele die perinatally, and homozygous TRAPα-*ShBle-LacZ* embryos are small and have cardiac outflow tract and endocardial cushion defects[38]. Therefore, TRAPα likely plays a role in the translocation of other secreted proteins that play important roles in embryonic development. Defining specific features of translocated proteins that confer TRAPα dependence[14,39] will facilitate the identification of additional TRAPα client proteins and the elucidation of other biological functions of TRAPα.

Supplementary Information is linked to the online version of the paper.

Acknowledgements: This work was supported by American Heart Association Postdoctoral Fellowship Award 14POST20390031 (O.A.I.); NIH R01DK120047 (L.Q.), R01DK111174 (L.Q., P.A., and M.L.), R01DK048280 (P.A.), and R01DK088856 (M.L.); National Natural Science Foundation of China grants 81070629, 81570699, 81620108004, and 81370895 (M.L.); and NIH R01AG041177, American Cancer Society Research Scholar Grant 119640-RSG-10-132-01-DDC, and American Heart Association Innovative Research Grant 11IRG5170009 (P.J.H.). We acknowledge support from the Michigan Diabetes Research Center Morphology Core (NIH P30 DK020572) and thank Roland Stein for comments on the manuscript.

Author contributions: Conceived of the project: O.A.I., P.A., M.L., P.J.H.; performed experiments: X.L., O.A.I., L.H., K.J.D., J.Y., J.C., H.-J.S., J.X.; analyzed data: X.L., O.A.I., L.H., K.J.D., J.C., S.F., H.-J.S., L.Q., P.A., M.L., P.J.H.; wrote the manuscript: P.A., M.L., P.J.H.

Competing interests: The authors declare no competing interests.

Materials and correspondence: Requests for materials and other correspondence should be addressed to Patrick J. Hu (patrick.j.hu@vumc.org).

Figure 1

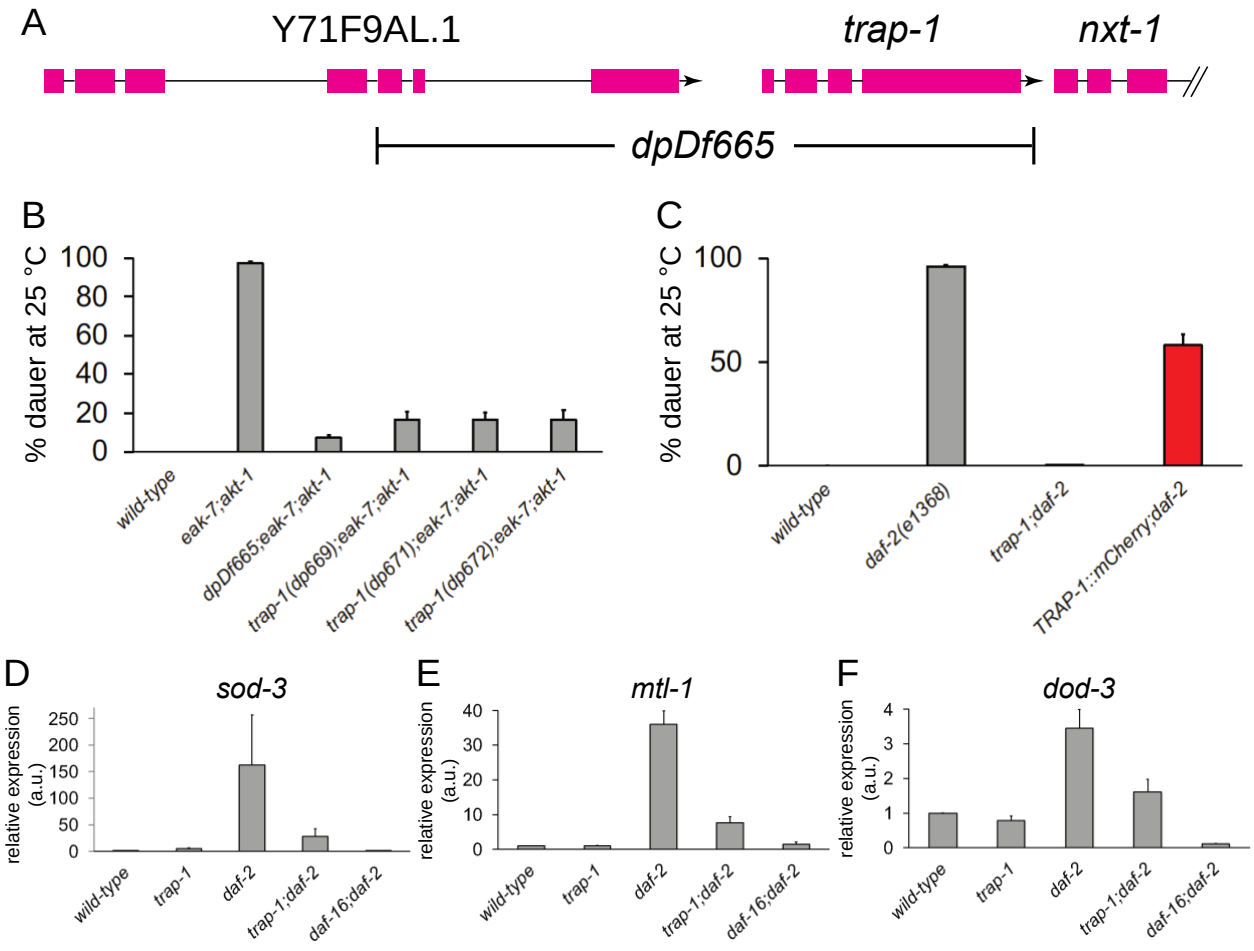

Figure 1. *trap-1* loss-of-function enhances DAF-2/InsR signaling. A. Schematic of the *trap-1* genomic region and the *dpDf665* deletion allele identified in a genetic screen. B. *trap-1* null alleles *dp669, dp671,* and *dp672* (Figure S1) phenocopy dauer suppression caused by *dpDf665* deletion. C. The *trap-1(dp672)* null mutation suppresses the dauer-constitutive phenotype of a *daf-2/InsR* loss-of-function mutant, and a TRAP-1::mCherry fusion protein is functional. D.-F. The *trap-1(dp672)* null mutation inhibits the expression of the DAF-16/FoxO target genes D. *sod-3,* E. *mtl-1,* and F. *dod-3.* a.u., arbitrary units.

Figure 2

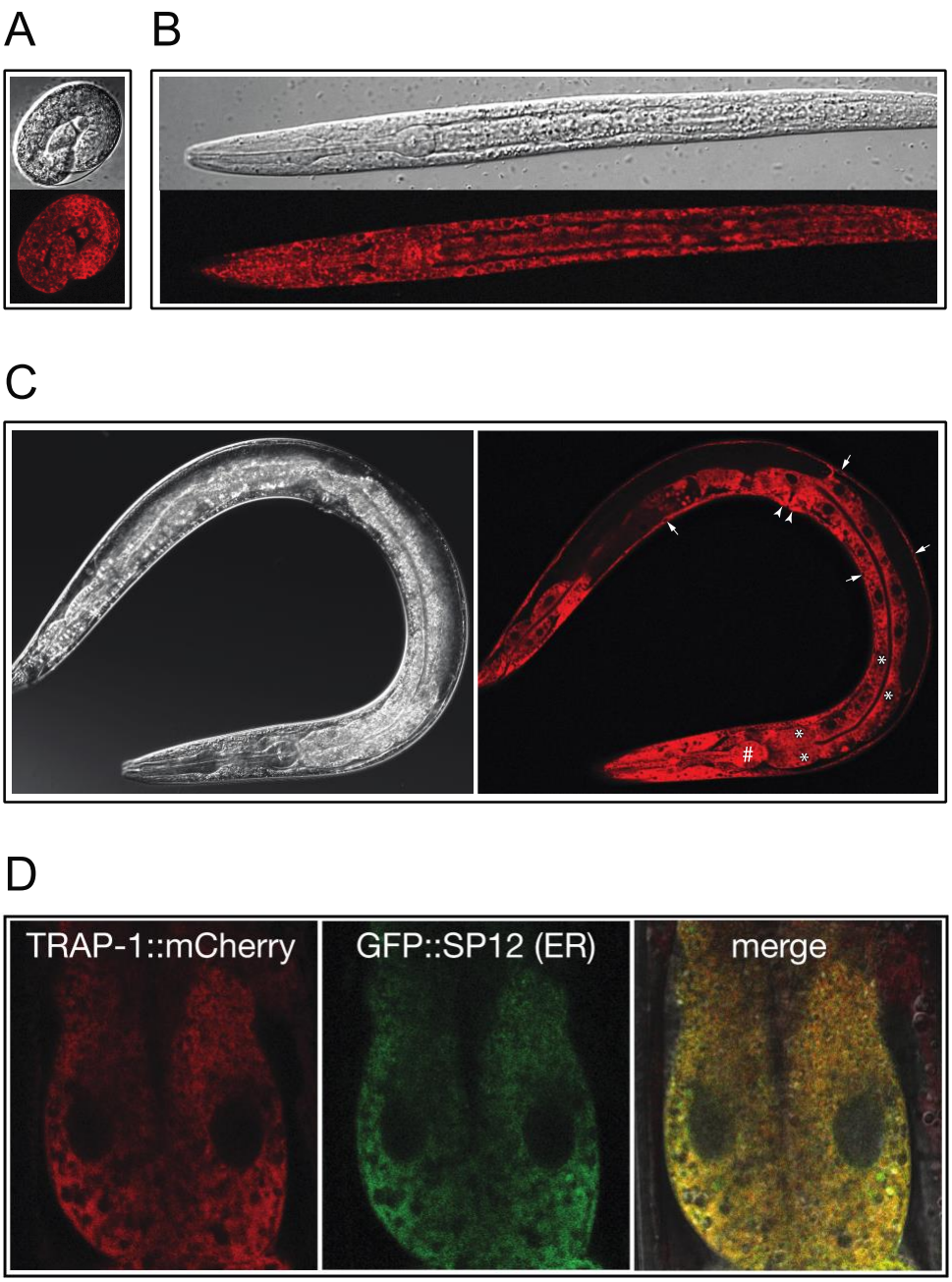

Figure 2. Spatiotemporal expression of a functional TRAP-1::mCherry fusion protein. TRAP-1::mCherry is expressed widely in A. embryos, B. larvae, and C. adult animals. Differential interference contrast (upper panel in A. and B., left panel in C.) and fluorescence (lower

256 panel in A. and B., right panel in C.) images are shown of representative animals. In adults

257 (C.), TRAP-1::mCherry is expressed in the pharynx (hashtag), intestine (asterisks),

258 hypodermis (arrows), and vulva (arrowheads). D. TRAP-1::mCherry colocalizes with the ER

259 signal peptidase GFP-SP12. Two anterior intestinal cells are shown.

Figure 3

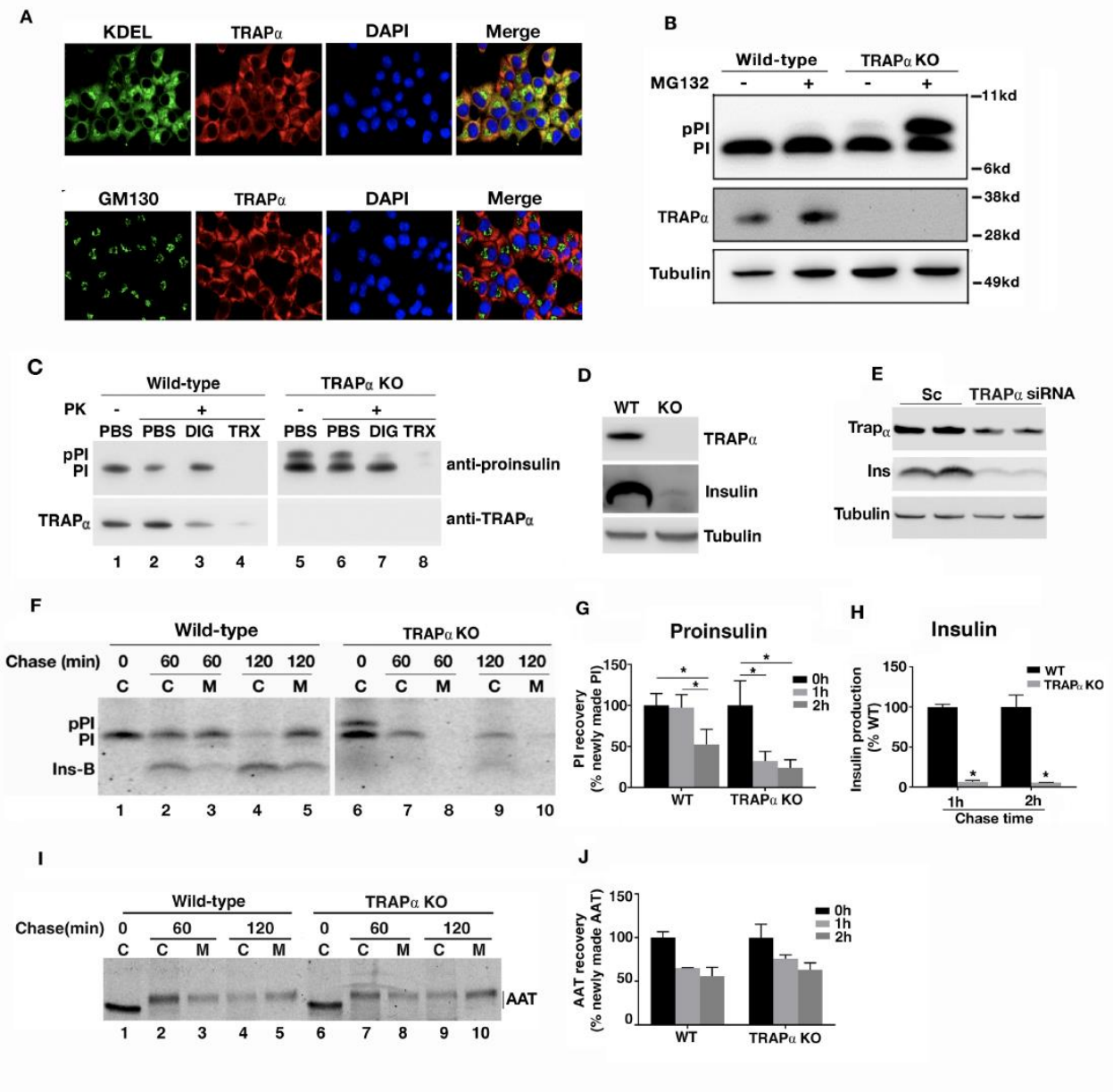

Figure 3. TRAPα promotes preproinsulin ER translocation, insulin biogenesis, and insulin secretion in INS 832/13 cells. A. Immunostaining of INS 832/13 cells with anti-TRAPα antibodies reveals colocalization with ER proteins recognized by anti-KDEL antibodies (upper panels) but not with the Golgi protein GM130 (lower panels). Nuclei are stained with

DAPI. B. SDS-PAGE and anti-proinsulin immunoblotting of lysates from INS 832/13 wild-type or TRAPα KO cells. Cells were untreated or treated with the proteasome inhibitor MG132 as indicated. Abbreviations: pPI, preproinsulin; PI, proinsulin. C. SDS-PAGE and anti-proinsulin immunoblotting of lysates from INS 832/13 wild-type or TRAPα KO cells after pretreatment with phosphate-buffered saline (PBS), digitonin (DIG), or Triton X-100 (TRX) and subsequent exposure to Proteinase K (PK). D. SDS-PAGE and anti-insulin immunoblotting of lysates from INS 832/13 wild-type and TRAPα KO cells. E. SDS-PAGE and anti-insulin immunoblotting of lysates from INS 832/13 wild-type cells that were transfected with either scrambled (Sc) or TRAPα siRNAs. Duplicate samples were run. F. SDS-PAGE of anti-insulin immunoprecipitates of cell lysates (C) or conditioned media (M) from INS 832/13 wild-type or TRAPα KO cells after pulse-labeling with ^{35}S-Met/Cys and chase for the indicated times. Abbreviations: pPI, preproinsulin; PI, proinsulin; Ins-B, insulin. Quantification of total proinsulin and insulin (C + M) is shown in G. and H., respectively. I. SDS-PAGE of anti-α1-antitrypsin (AAT) immunoprecipitates of cell lysates (C) or conditioned media (M) from INS 832/13 wild-type or TRAPα KO cells after pulse-labeling and chase as described for F. INS 832/13 wild-type or TRAPα KO cells were transfected with a plasmid encoding AAT 48 hours prior to pulse-labeling. J. Quantification of total AAT (C + M) at the indicated time points.

Figure 4

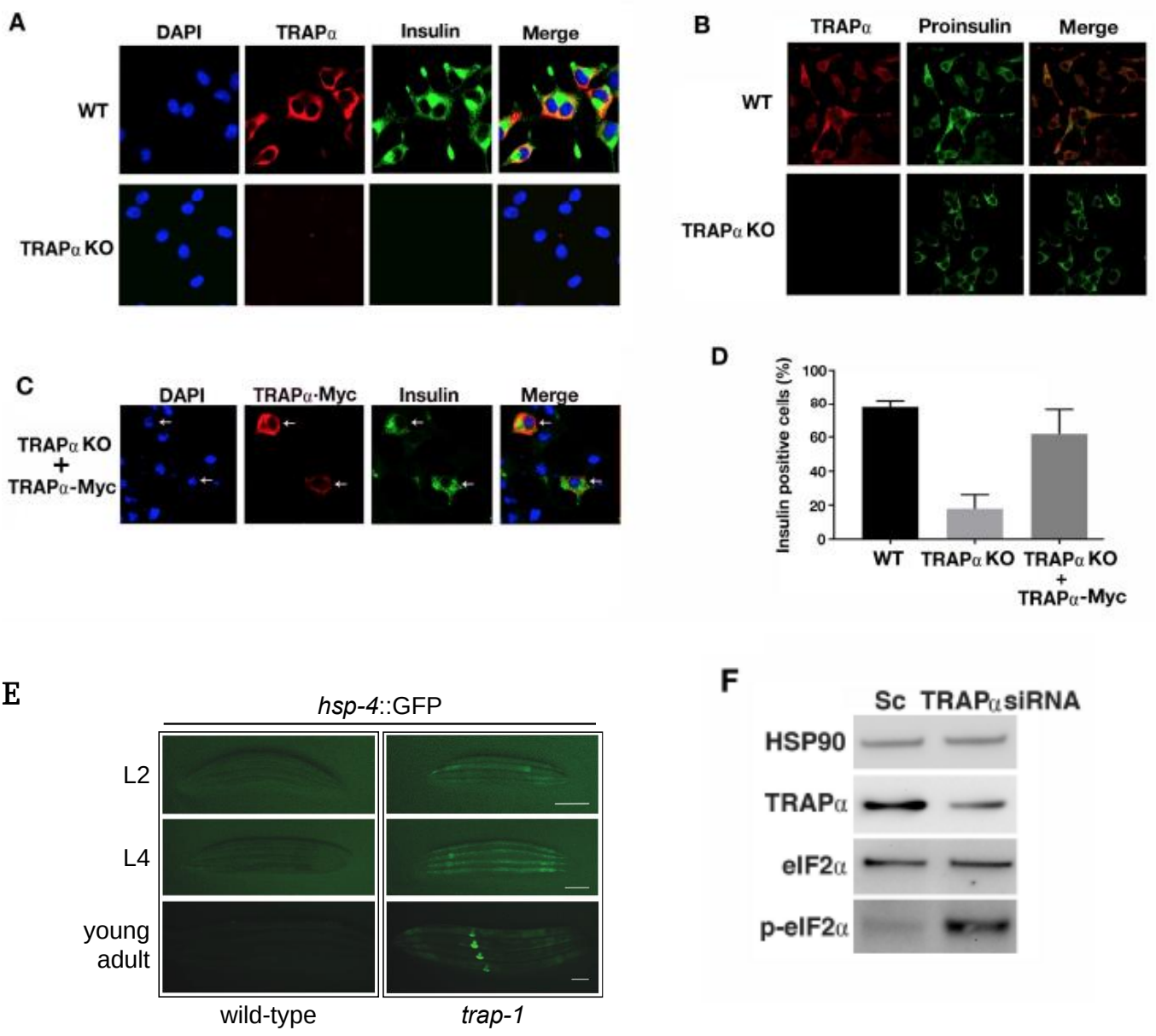

Figure 4. TRAPα promotes insulin biosynthesis and reduces ER stress. A. Immunostaining of INS832/13 wild-type (WT) or TRAPα KO cells with anti-TRAPα and A. anti-insulin or B. anti-proinsulin antibodies. Nuclei are stained with DAPI. C. Immunostaining of TRAPα KO

295 cells with anti-Myc and anti-insulin antibodies after transfection with a plasmid encoding a
296 Myc-tagged TRAPα cDNA. Nuclei are stained with DAPI. D. Quantification of insulin-
297 positive cells in INS832/13 wild-type, TRAPα KO, and TRAPα KO cells expressing
298 exogenous Myc-tagged TRAPα. E. Expression of the ER stress reporter *hsp-4*::GFP in second
299 (L2) and fourth stage (L4) larvae and young adult wild-type (left panels) and *trap-1(dp672)*
300 null mutant (right panels) animals. At each stage, images of wild-type and *trap-1* mutant
301 animals were captured with equivalent exposure times. Scale bar: 100 microns. F. SDS-PAGE
302 and anti-phospho-Ser51-eIF2 immunoblotting of lysates from INS 832/13 wild-type cells that
303 were transfected with either scrambled (Sc) or TRAPα siRNA as indicated.

REFERENCES

1 Prehn, S. *et al.* Structure and biosynthesis of the signal-sequence receptor. *Eur J Biochem* **188**, 439-445 (1990).

2 Replication, D. I. G. *et al.* Genome-wide trans-ancestry meta-analysis provides insight into the genetic architecture of type 2 diabetes susceptibility. *Nat Genet* **46**, 234-244, doi:10.1038/ng.2897 (2014).

3 Fielenbach, N. & Antebi, A. C. elegans dauer formation and the molecular basis of plasticity. *Genes Dev* **22**, 2149-2165, doi:10.1101/gad.1701508 (2008).

4 Murphy, C. T. & Hu, P. J. Insulin/insulin-like growth factor signaling in C. elegans. *WormBook*, 1-43, doi:10.1895/wormbook.1.164.1 (2013).

5 Delaney, C. E., Chen, A. T., Graniel, J. V., Dumas, K. J. & Hu, P. J. A histone H4 lysine 20 methyltransferase couples environmental cues to sensory neuron control of developmental plasticity. *Development* **144**, 1273-1282, doi:10.1242/dev.145722 (2017).

6 Dumas, K. J. *et al.* Unexpected role for dosage compensation in the control of dauer arrest, insulin-like signaling, and FoxO transcription factor activity in Caenorhabditis elegans. *Genetics* **194**, 619-629, doi:10.1534/genetics.113.149948 (2013).

7 Itani, O. A., Flibotte, S., Dumas, K. J., Moerman, D. G. & Hu, P. J. Chromoanasynthetic Genomic Rearrangement Identified in a N-Ethyl-N-Nitrosourea (ENU) Mutagenesis Screen in Caenorhabditis elegans. *G3 (Bethesda)* **6**, 351-356, doi:10.1534/g3.115.024257 (2015).

8 Alam, H. *et al.* EAK-7 controls development and life span by regulating nuclear DAF-16/FoxO activity. *Cell Metab* **12**, 30-41, doi:10.1016/j.cmet.2010.05.004 (2010).

9 Hu, P. J. Dauer. *WormBook*, 1-19, doi:10.1895/wormbook.1.144.1 (2007).

10 Murphy, C. T. *et al.* Genes that act downstream of DAF-16 to influence the lifespan of Caenorhabditis elegans. *Nature* **424**, 277-283, doi:10.1038/nature01789 (2003).

11 Wiedmann, M., Kurzchalia, T. V., Hartmann, E. & Rapoport, T. A. A signal sequence receptor in the endoplasmic reticulum membrane. *Nature* **328**, 830-833, doi:10.1038/328830a0 (1987).

12 Hartmann, E. *et al.* A tetrameric complex of membrane proteins in the endoplasmic reticulum. *Eur J Biochem* **214**, 375-381 (1993).

13 Xu, N. *et al.* The FATP1-DGAT2 complex facilitates lipid droplet expansion at the ER-lipid droplet interface. *J Cell Biol* **198**, 895-911, doi:10.1083/jcb.201201139 (2012).

14 Fons, R. D., Bogert, B. A. & Hegde, R. S. Substrate-specific function of the translocon-associated protein complex during translocation across the ER membrane. *J Cell Biol* **160**, 529-539, doi:10.1083/jcb.200210095 (2003).

15 Snapp, E. L., Reinhart, G. A., Bogert, B. A., Lippincott-Schwartz, J. & Hegde, R. S. The organization of engaged and quiescent translocons in the endoplasmic reticulum of mammalian cells. *J Cell Biol* **164**, 997-1007, doi:10.1083/jcb.200312079 (2004).

16 Pfeffer, S. *et al.* Structure and 3D arrangement of endoplasmic reticulum membrane-associated ribosomes. *Structure* **20**, 1508-1518, doi:10.1016/j.str.2012.06.010 (2012).

17 Menetret, J. F. *et al.* Architecture of the ribosome-channel complex derived from native membranes. *J Mol Biol* **348**, 445-457, doi:10.1016/j.jmb.2005.02.053 (2005).

18 Menetret, J. F. *et al.* Single copies of Sec61 and TRAP associate with a nontranslating mammalian ribosome. *Structure* **16**, 1126-1137, doi:10.1016/j.str.2008.05.003 (2008).

19 Pfeffer, S. *et al.* Dissecting the molecular organization of the translocon-associated protein complex. *Nat Commun* **8**, 14516, doi:10.1038/ncomms14516 (2017).

20 Pierce, S. B. *et al.* Regulation of DAF-2 receptor signaling by human insulin and ins-1, a member of the unusually large and diverse C. elegans insulin gene family. *Genes Dev* **15**, 672-686, doi:10.1101/gad.867301 (2001).

21 Hung, W. L., Wang, Y., Chitturi, J. & Zhen, M. A Caenorhabditis elegans developmental decision requires insulin signaling-mediated neuron-intestine communication. *Development* **141**, 1767-1779, doi:10.1242/dev.103846 (2014).

22 Patel, D. S. *et al.* Clustering of genetically defined allele classes in the Caenorhabditis elegans DAF-2 insulin/IGF-1 receptor. *Genetics* **178**, 931-946, doi:10.1534/genetics.107.070813 (2008).

23 Kimura, K. D., Tissenbaum, H. A., Liu, Y. & Ruvkun, G. daf-2, an insulin receptor-like gene that regulates longevity and diapause in Caenorhabditis elegans. *Science* **277**, 942-946 (1997).

24 Krook, A. *et al.* Molecular scanning of the insulin receptor gene in syndromes of insulin resistance. *Diabetes* **43**, 357-368 (1994).

25 Krook, A., Moller, D. E., Dib, K. & O'Rahilly, S. Two naturally occurring mutant insulin receptors phosphorylate insulin receptor substrate-1 (IRS-1) but fail to mediate the biological effects of insulin. Evidence that IRS-1 phosphorylation is not sufficient for normal insulin action. *J Biol Chem* **271**, 7134-7140 (1996).

26 Scott, B. A., Avidan, M. S. & Crowder, C. M. Regulation of hypoxic death in C. elegans by the insulin/IGF receptor homolog DAF-2. *Science* **296**, 2388-2391, doi:10.1126/science.1072302 (2002).

27 Hamer, I. *et al.* An arginine to cysteine(252) mutation in insulin receptors from a patient with severe insulin resistance inhibits receptor internalisation but preserves signalling events. *Diabetologia* **45**, 657-667, doi:10.1007/s00125-002-0798-5 (2002).

28 Barbetti, F. *et al.* Detection of mutations in insulin receptor gene by denaturing gradient gel electrophoresis. *Diabetes* **41**, 408-415 (1992).

29 Wertheimer, E., Barbetti, F., Muggeo, M., Roth, J. & Taylor, S. I. Two mutations in a conserved structural motif in the insulin receptor inhibit normal folding and intracellular transport of the receptor. *J Biol Chem* **269**, 7587-7592 (1994).

30 Maggi, D. & Cordera, R. Cys 786 and Cys 776 in the posttranslational processing of the insulin and IGF-I receptors. *Biochem Biophys Res Commun* **280**, 836-841, doi:10.1006/bbrc.2000.4224 (2001).

31 Nakamura, N. *et al.* Characterization of a cis-Golgi matrix protein, GM130. *J Cell Biol* **131**, 1715-1726 (1995).

32 Nagasawa, K., Higashi, T., Hosokawa, N., Kaufman, R. J. & Nagata, K. Simultaneous induction of the four subunits of the TRAP complex by ER stress accelerates ER degradation. *EMBO Rep* **8**, 483-489, doi:10.1038/sj.embor.7400933 (2007).

33 Calfon, M. *et al.* IRE1 couples endoplasmic reticulum load to secretory capacity by processing the XBP-1 mRNA. *Nature* **415**, 92-96, doi:10.1038/415092a (2002).

34 Harding, H. P., Zhang, Y. & Ron, D. Protein translation and folding are coupled by an endoplasmic-reticulum-resident kinase. *Nature* **397**, 271-274, doi:10.1038/16729 (1999).

35 Liu, M. *et al.* Proinsulin misfolding and diabetes: mutant INS gene-induced diabetes of youth. *Trends Endocrinol Metab* **21**, 652-659, doi:10.1016/j.tem.2010.07.001 (2010).

36 Webb, G. C., Akbar, M. S., Zhao, C. & Steiner, D. F. Expression profiling of pancreatic beta cells: glucose regulation of secretory and metabolic pathway genes. *Proc Natl Acad Sci U S A* **97**, 5773-5778, doi:10.1073/pnas.100126597 (2000).

37 Hassler, J. R. *et al.* The IRE1alpha/XBP1s Pathway Is Essential for the Glucose Response and Protection of beta Cells. *PLoS Biol* **13**, e1002277, doi:10.1371/journal.pbio.1002277 (2015).

38 Mesbah, K., Camus, A., Babinet, C. & Barra, J. Mutation in the Trapalpha/Ssr1 gene, encoding translocon-associated protein alpha, results in outflow tract morphogenetic defects. *Mol Cell Biol* **26**, 7760-7771, doi:10.1128/MCB.00913-06 (2006).

39 Nguyen, D. *et al.* Proteomics reveals signal peptide features determining the client specificity in human TRAP-dependent ER protein import. *Nat Commun* **9**, 3765, doi:10.1038/s41467-018-06188-z (2018).

40 Gems, D. *et al.* Two pleiotropic classes of daf-2 mutation affect larval arrest, adult behavior, reproduction and longevity in Caenorhabditis elegans. *Genetics* **150**, 129-155 (1998).

412 ## METHODS

413

414 **Generation and maintenance of *C. elegans* strains:** Strains were maintained on standard
415 nematode growth media (NGM) plates seeded with *Escherichia coli* OP50. Double and triple
416 mutant strains were constructed using conventional methods. *trap-1* mutant alleles were
417 generated using CRISPR/Cas9-based genome editing[1]. Two guide RNAs complementary to
418 sequences in exon 2 were used. Molecular analysis of *trap-1* mutants is described in Figure
419 S1. DNA encoding a mCherry epitope tag was inserted in-frame at the 3' end of the *trap-1*
420 open reading frame using CRISPR/Cas9-based homology-directed genome editing as
421 described[2]. Red fluorescent animals were isolated, and the mCherry insertion was verified by
422 Sanger sequencing of PCR products spanning the insertion site.

423

424 **Genetic screen for modifiers of *C. elegans* DAF-2/InsR signaling:** The suppressor of *eak-*
425 *7;akt-1* (*seak*) screen was performed by mutagenizing *eak-7;akt-1* double mutants with *N*-
426 ethyl-*N*-nitrosourea (ENU) and screening for rare animals in the F_2 generation that did not
427 arrest as dauers as described[3]. Genomic DNA isolated from *eak-7;akt-1* suppressor strains was
428 sequenced and analyzed as described[3].

429

430 **Dauer arrest assays:** Dauer arrest assays were performed at 25°C as previously described[4].

431

432 **Real-time quantitative PCR (qPCR):** qPCR was performed as previously described[5].

433

434 ***C. elegans* fluorescence microscopy:** Animals were mounted on slides layered with a thin 3%
435 agarose pad containing 25 mM sodium azide. Images were captured on a Leica inverted SP5
436 X inverted confocal microscope using LAS AF software (Leica).

437

438 **Reagents:** Rat monoclonal anti-KDEL and rabbit monoclonal anti-GM130 antibodies were
439 from Abcam (ab50601 and ab52649, respectively). Rabbit polyclonal anti-TRAPα antibodies
440 were from Novus Biologicals (NBP1-86912). A mouse monoclonal antibody that recognizes a
441 human proinsulin C-peptide—A-chain junction peptide (GSLQKRGIVE) was raised by
442 Abmart. Mouse monoclonal anti-tubulin antibodies were from Sigma (T5168). Guinea pig
443 polyclonal anti-porcine insulin antibodies were from Millipore. Rabbit polyclonal anti-α1-
444 antitrypsin (AAT) antibodies were from Dako (A001202-2). Rabbit polyclonal anti-HSP90
445 (#4874S), anti-eIF2 (#9722S), and anti-phospho-Ser51 eIF2 antibodies (#9721) were from Cell
446 Signaling. ^{35}S-Met/Cys was from ICN. Dithiothreitol (DTT), protein A-agarose, digitonin, N-
447 ethylmaleimide (NEM), and other chemical reagents were from Sigma-Aldrich. 4-12%
448 gradient SDS-polyacrylamide gel electrophoresis (SDS-PAGE) was performed using NuPage
449 gels from Thermo Fisher. Met/Cys-deficient Dulbecco's modified Eagle's medium (DMEM)
450 and all other tissue culture reagents were from Invitrogen. A cDNA encoding Myc epitope-
451 tagged human TRAPα was synthesized by Integrated DNA Technologies (IDT) and was
452 subcloned into the pTarget mammalian expressing vector (Promega).

453 **Manipulating TRAPα expression in INS832/13 cells:** INS832/13 cells lacking TRAPα were
454 generated using CRISPR/Cas9-mediated genome editing[6]. Single guide RNAs (sgRNAs) were
455 designed using guide design resources available on the Zhang Lab web site
456 (https://zlab.bio/guide-design-resources). Oligonucleotides corresponding to 5' -
457 CACCGTCTGCACTCGGTGAAGCTTC - 3' 20-nt guide sequences were annealed and ligated
458 into pSpCas9(BB)-2A-Puro (PX462) v2.0 vector as described[6]. This plasmid was transfected
459 into INS832/13 cells using Lipofectamine 2000 (Thermo Fisher). 48 hours after transfection,
460 cells were plated and cultured with RPMI growth medium containing 1 μg/ml puromycin.
461 Puromycin-resistant clones were screened for loss of TRAPα ("TRAPα KO") by
462 immunoblotting with anti-TRAPα antibodies. To re-express TRAPα, TRAPα KO cells were
463 transiently transfected with a plasmid encoding Myc-tagged human TRAPα. 48 hours after
464 transfection, insulin content was assayed by immunofluorescence. To reduce TRAPα
465 expression by RNAi, INS832/13 cells were transfected with 20nM TRAPα targeting siRNA
466 (Assay ID 219062, Thermo Fisher) or Negative Control siRNA (AM4611, Thermo Fisher)
467 using Lipofectamine RNAiMAX (Invitrogen). 48 hours after transfection, knockdown
468 efficiency was evaluated by immunoblotting using anti-TRAPα antibodies.
469
470 **Cell culture:** Cells were plated into 6-well plates one day before transfection. A total of 2 μg
471 plasmid DNA was transfected using Lipofectamine 2000 (Invitrogen). For metabolic labeling,
472 cells were pulse-labeled with ^{35}S-Met/Cys for 15 minutes, washed, and chased with label-free
473 media for 0, 60, or 120 minutes as indicated. Immediately thereafter, media and cell lysate

474 were immunoprecipitated with anti-insulin or anti-AAT antibodies, and immunoprecipitates
475 were subjected to 4-12% gradient SDS-PAGE under reducing conditions. Preproinsulin,
476 proinsulin, insulin, and AAT were analyzed using a Typhoon Phosphorimager (GE
477 Healthcare). Band intensities were quantified using NIH ImageJ. For selective plasma
478 membrane permeabilization and Proteinase K digestion, cells were incubated on ice with
479 phosphate-buffered saline (PBS), with or without 10 μg/ml Proteinase K, 0.01% digitonin, or
480 1% Triton X-100 as indicated for 30 minutes. Cells were harvested, boiled in SDS sample
481 buffer, and analyzed by immunoblotting with anti-proinsulin antibodies.
482
483 **Immunofluorescence:** Cells were permeabilized with 0.5% Triton X-100, fixed with
484 formaldehyde, blocked, and incubated with anti-TRAPα, anti-KDEL, anti-GM130, anti-
485 insulin, anti-proinsulin, or anti-Myc antibodies. After incubation with fluorophore-
486 conjugated secondary antibodies, specimens were imaged with an Olympus FV500 confocal
487 microscope.
488
489 **Immunoblotting:** Cell lysates were boiled in sample buffer containing 100 mM DTT for five
490 minutes, resolved by 4–12% gradient SDS-PAGE, and transferred to nitrocellulose. Primary
491 antibodies were used at 1:1000 dilution in TBST (0.1% Tween 20) plus 5% bovine serum
492 albumin, with the exception of anti-HSP90, which was used at 1:2000 dilution. Secondary
493 antibodies [goat anti-rabbit IgG HRP, goat anti-mouse IgG HRP (both from Biorad), and goat
494 anti-guinea pig IgG HRP (Jackson ImmunoResearch)] were used at 1:5000 dilution. Imaging

was performed after incubation with Clarity Western ECL Substrate (Bio-Rad #1705061) according to the manufacturer's instructions.

Statistical analyses: Statistical analyses were carried out by Student's t-test or one-way ANOVA using GraphPad Prism 7.

***hsp-4p*::GFP reporter assay**: Wild-type and *trap-1* mutant *C. elegans* harboring an integrated *hsp-4p*::GFP transgene[7] were harvested, incubated in alkaline hypochlorite [500 mM NaOH and 1.2% (v/v) hypochlorite], and vortexed to isolate eggs. Eggs were washed two times with M9 buffer solution and incubated at 20°C on standard NGM plates seeded with *E. coli* OP50. Animals were imaged at L2 larval, L4 larval, and young adult stages on a Leica SP5 X confocal microscope equipped with LAS AF software. Three experimental replicates yielded similar results.

Data availability: The data that support the findings of this study are available from the corresponding author upon reasonable request.

REFERENCES

1 Friedland, A. E. *et al.* Heritable genome editing in *C. elegans* via a CRISPR-Cas9 system. *Nat Methods* **10**, 741-743, doi:10.1038/nmeth.2532 (2013).

2 Paix, A., Folkmann, A., Rasoloson, D. & Seydoux, G. High Efficiency, Homology-Directed Genome Editing in *Caenorhabditis elegans* Using CRISPR-Cas9 Ribonucleoprotein Complexes. *Genetics* **201**, 47-54, doi:10.1534/genetics.115.179382 (2015).

3 Dumas, K. J. *et al.* Unexpected role for dosage compensation in the control of dauer arrest, insulin-like signaling, and FoxO transcription factor activity in *Caenorhabditis elegans*. *Genetics* **194**, 619-629, doi:10.1534/genetics.113.149948 (2013).

4 Hu, P. J., Xu, J. & Ruvkun, G. Two membrane-associated tyrosine phosphatase homologs potentiate *C. elegans* AKT-1/PKB signaling. *PLoS Genet* **2**, e99, doi:10.1371/journal.pgen.0020099 (2006).

5 Chen, A. T. *et al.* Longevity Genes Revealed by Integrative Analysis of Isoform-Specific *daf-16/FoxO* Mutants of *Caenorhabditis elegans*. *Genetics* **201**, 613-629, doi:10.1534/genetics.115.177998 (2015).

6 Ran, F. A. *et al.* Genome engineering using the CRISPR-Cas9 system. *Nat Protoc* **8**, 2281-2308, doi:10.1038/nprot.2013.143 (2013).

7 Calfon, M. *et al.* IRE1 couples endoplasmic reticulum load to secretory capacity by processing the XBP-1 mRNA. *Nature* **415**, 92-96, doi:10.1038/415092a (2002).